Mechanism Responsible for Initiating Carbon Nanotube Vacuum Breakdown

N. Y. Huang,[1] J. C. She,[1] Jun Chen,[1] S. Z. Deng,[1] N. S. Xu,[1,*] H. Bishop,[2] S. E. Huq,[3] L. Wang,[3] D. Y. Zhong,[4] E. G. Wang,[4] and D. M. Chen[5]

[1]*State Key Lab of Optoelectronic Materials and Technologies, and Guangdong Province Key Laboratory of Display Materials and Technologies, Sun Yat-sen (Zhongshan) University, Guangzhou, People's Republic of China*

[2]*Printable Field Emitters Ltd., Rutherford Appleton Laboratory, Didcot, OX11 0QX, United Kingdom*

[3]*Central Microstructure Facility, Rutherford Appleton Laboratory, Didcot, OX11 0QX, United Kingdom*

[4]*State Key Laboratory for Surface Science Physics, Institute of Physics, Chinese Academy of Science, Beijing 100080, People's Republic of China*

[5]*Rowland Institute at Harvard, Harvard University, Cambridge, Massachusetts 02142, USA*

(Received 14 April 2004; published 11 August 2004)

We report a physical mechanism responsible for initiating a vacuum breakdown process of a single carbon nanotube (CNT) during field emission. A quasidynamic method has been developed to simulate the breakdown process and calculate the critical field, critical emission current density and critical temperature beyond which thermal runaway occurs before the CNT temperature reaches its melting point. This model is in good agreement with experiments carried out with a single CNT on a silicon microtip.

DOI: 10.1103/PhysRevLett.93.075501 PACS numbers: 61.48.+c, 73.21.–b, 79.70.+q, 85.45.Db

Carbon nanotubes (CNTs) have attracted considerable attention not only because of their unique physical properties, but also their potential applications [1,2]. For example, field electron emission from CNTs already finds applications in flat panel displays [3] and miniature high-brightness electron sources for both electron microscope [4] and parallel e-beam lithography system [5]. One major technical challenge is to have an acceptable high upper emission current density, but a CNT operating at such a current level often is unstable and may experience a vacuum breakdown, which is often catastrophic and can lead to the malfunction of a device. So far, there is not a clear understanding of the physical mechanism responsible for initiating such a breakdown. Bonard *et al.* [6] attributed the failure of a multiwall CNT to resistive heating at the contact to substrate. Wang *et al.* [7] suggested the instability in emission current was due to the structural damage during emission. Emitting CNTs will involve a self-heating process [8–10], which may result in subliming and melting of a CNT and ultimately causes a cathode-initiated vacuum breakdown process. This Letter addresses the physical mechanism responsible for initiating the breakdown process due to the self-heating.

We model a CNT as a one-dimensional object of length L in contact with a substrate at $x = 0$, and consider heat losses by radiation from the wall and the cap of CNT, and by heat conduction to the substrate (Fig. 1). The time-independent heat equation may be expressed as

$$Q - \pi r^2(q_x - q_{x+dx}) - 2\pi r dx\sigma(T_x^4 - T_0^4) = 0, \quad (1)$$

where Q is the heat source, r is the radius of CNT, q_x is the heat flux, T_x is the temperature, and all at x point, T_0 is the ambient temperature, σ is the Stefan-Boltzmann constant (we assume emissivity = 1). Considering only Joule heating in a CNT, $Q = I^2R(T_x)L^{-1}dx$, where I is the emission current, R the resistance of CNT. Using the expression of Q and the Fourier heat conduction law $q = -k\nabla T$ (k is the heat conduction coefficient), Eq. (1) becomes

$$\pi r^2 k\frac{\partial^2 T_x}{\partial x^2}dx - 2\pi r dx\sigma(T_x^4 - T_0^4) + I^2R(T_x)L^{-1}dx = 0. \quad (2)$$

Heat loss by radiation from the cap of CNT can be determined by

$$\frac{\partial T_A}{\partial x} = -\sigma k^{-1}(T_A^4 - T_0^4), \quad (3)$$

where T_A is the temperature of the apex of CNT.

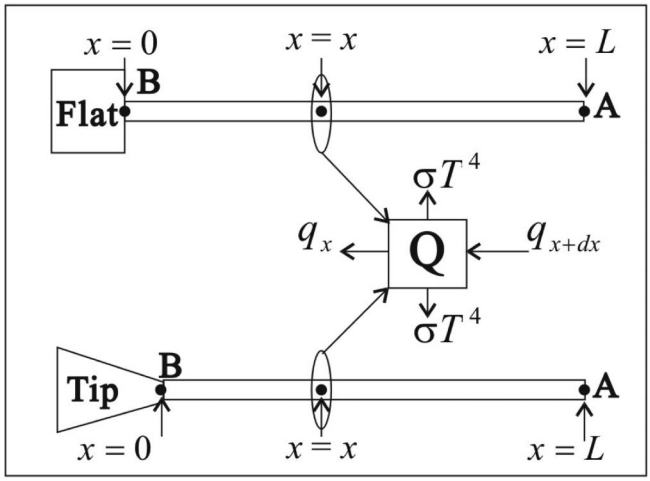

FIG. 1. Illustrating two emission regimes modeled.

Meanwhile, heat loss to substrate is dependent of its geometry. For a flat substrate, which may be assumed as a heat sink with a fixed temperature T_0, the temperature of CNT at $x = 0$ is

$$T_B = T_0. \tag{4a}$$

For a microtip substrate, we use an empirical expression

$$T_B = \lambda \pi r^2 k \frac{\partial T_B}{\partial x} + T_0, \tag{4b}$$

where λ is a constant, determined by the shape of microtip and the contact resistance between microtip and CNT, and can usually be chosen to match the experimental data. Solving the heat Eq. (2) with the boundary condition expressions (3), (4a), and (4b), the temperature T_x especially T_A can be obtained for a predetermined value of emission current. However, it is impossible to solve Eq. (2) explicitly, since R is strongly influenced by temperature T.

The expression for R as a function of T is dependent on electron scattering mechanism. Previously Purcell *et al.* [9] assumed that $R(T) = R_0(1 - \alpha T)$, where α is the resistance temperature coefficient, which can be chosen to match with experimental data, and R_0 is the resistance at 300 K. The decrease in R with increasing T was attributed to different conduction mechanisms, such as hopping along thermally activated defect sites [11,12]. However, R should not decrease indefinitely, and some mechanisms such as electron-phonon scattering can make R increase with T [13]. Thus we assume a new expression

$$R(T) = R_0(1 - \alpha T + \beta T^{3/2}), \tag{5}$$

where α and β may be chosen to match with experimental data. With specific boundary conditions, by solving Eqs. (2) and (5), both T_A versus I and R versus I can be obtained. Excellent fit has been found between Purcell's experimental data [9,10] and Eq. (5). Further, very good agreement has also been found between the prediction from Eq. (5) and experimental data reported by Collins *et al.* [14], who studied the electrical breakdown of a CNT in air.

The current flowing in a CNT in emission also varies with temperature due to the heating at the apex of CNT, which causes a rise in emission current. Under such circumstance thermal equilibrium will not be reached, if there are no heat losses. Then this positive feedback process will continue until a CNT reaches its melting point. Since there are heat losses, thermal equilibrium will be established under certain conditions. Our present task is to find the critical conditions, which define where a thermal equilibrium can be maintained and where an uncontrollable process will initiate. In the latter case, the process takes place rapidly and will not be controllable under direct current conditions. Such a thermal runaway is the initiation of a vacuum breakdown process.

The current flowing in a CNT equals to its field emission current, given by Murphy and Good [15]:

$$\begin{aligned} j(E, T_A) = \int_{-w_a}^{w_1} \frac{4\pi m e k_B T_A}{h^3} \Bigg\{ & 1 + \exp\left[\frac{8\pi (2m|w|^3)^{1/2}}{3heE} \upsilon(Y) \right] \Bigg\}^{-1} \times \ln\Bigg\{ 1 + \exp\left[\frac{-(w - \xi)}{k_B T_A} \right] dw \Bigg\} + \int_{-w_1}^{\infty} \frac{4\pi m e k_B T_A}{h^3} \\ & \times \ln\Bigg\{ 1 + \exp\left[\frac{-(w - \xi)}{k_B T_A} \right] dw \Bigg\}, \end{aligned} \tag{6}$$

where $w_1 = -[e^3 E/(8\pi\varepsilon\varepsilon_0)]^{1/2}$, $Y = [e^3 E/(4\pi\varepsilon\varepsilon_0 w^2)]$, k_B is Boltzmann's constant, m is the effective mass of an electron, ξ is the Fermi energy, equal to $-\phi$, e is the electron charge, ε is the relative dielectric constant of the CNT, ε_0 is the dielectric constant of vacuum, and $\upsilon(Y)$ is the elliptic function.

The positive feedback process can be described as a dynamic feedback process [16]. An iterative algorithm can simulate this dynamic process (inset of Fig. 2). First, at a specific E_i, j_1 is calculated using expression (6) with $T_A = T_0$. The apex temperature T_1 resulted from passing j_1 is obtained using Eq. (2) with boundary conditions defined by Eqs. (3), (4a), and (4b). Usually T_1 is not the equilibrium temperature and will result in a new emission current density j_2, which may heat the CNT further to T_3. This process of calculation continues unless an equilibrium temperature is reached. One may repeat the iterative calculation for n times (often within $n = 300$), and assign the emission current density and the temperature as j_n and T_n, respectively. If $T_n = T_{n-1}$ and $T_n < T_m$, where T_m is the melting point of the CNT, the CNT reaches an

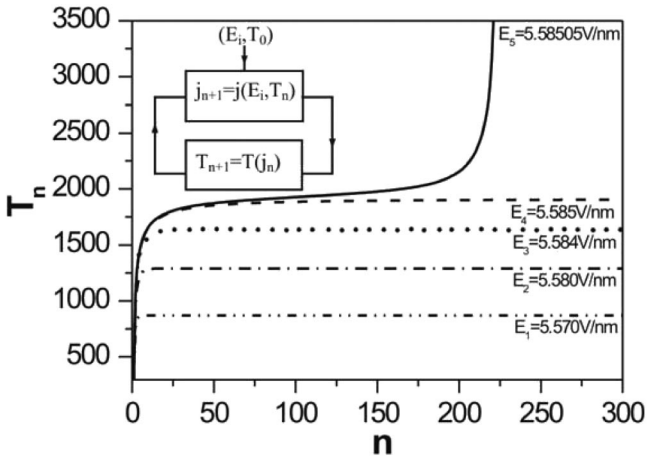

FIG. 2. T_n-n curves obtained using the quasidynamic simulation; the inset is the flow chart of the multiple loop feedback process.

equilibrium temperature and T_n is the final equilibrium apex temperature and j_n is the final equilibrium emission current density. Otherwise, if $T_n - T_{n-1} > 0$ and $(T_n - T_{n-1}) - (T_{n-1} - T_{n-2}) > 0$, the CNT cannot reach an equilibrium state, i.e., a thermal runaway will occur. A critical field E_c and a critical current density j_c may be found just before the runaway occurs. Above the critical field E_c, any slight increase in applied field will result in a thermal runaway event. As shown in Fig. 2, at an applied field lower than E_4, e.g., E_3, the CNT will reach an equilibrium temperature and at an applied field any slightly higher than E_4, the CNT will undergo a thermal runaway event. Thus, E_4 is the critical field, and the corresponding T_n andj_n ($n = 300$) are the critical apex temperature T_c and critical emission current density j_c, respectively.

We have first calculated $T_{c,}$ $j_{c,}$ and the critical field of a CNT on a flat substrate. The structural parameters of the CNT were given as $0.5 \leq L \leq 40$ μm and $r = 10$ nm. The other parameters were determined by matching with Purcell's experimental data [9] (Table I). We used the values of $1.7 \times 10^{-6} \sim 3.26 \times 10^{-5}$ Ωm and 100 W/mK for resistivity and thermal conductivity, respectively. These values have been found to fall in the range of most probable values reported for multiwalled CNTs so far [12,17–19]. Figure 3 shows the length dependence of the critical parameters. Following findings emerge: (i) Both critical field (E_c) and critical current density (j_c) nonlinearly decease with length (L). (ii) A minimum critical temperature (T_c) can be found at $L =$ 19 μm. For a CNT with $L > 19$ μm, T_c may be higher although I_c is smaller. Heat at the apex cannot be dissipated sufficiently to substrate since heat conduction is in inverse proportion to L. (iii) The critical gap field (E_{gap}), which is defined by $E_{\text{gap}} = E_c r/L$, varies with L in a way similar to that of I_c. (iv) T_c rises rapidly with decrease of CNT length [Fig. 3(b)]. Shorter CNT can lose more heat by heat conduction to substrate, thus T_c, at which a breakdown event is initiated, is likely to reach CNT's melting point. A mechanism responsible for this type of vacuum breakdown was fully described in elsewhere [20], in which case the current and thermal runaway may not be observed.

For a CNT on a Si microtip (Fig. 1), a temperature rise in the microtip cannot be neglected. The melting point of Si($\sim$1684 K) may be reached at a lower current density j_{c0}. Thus, failure of such an emitter may be initiated due to melting of Si microtip. We may refer it as a substrate-melting event. We have run a similar simulation to define critical conditions between such an event and a thermal runaway event. The temperatures of Si tip apex (equals to T_B indicated in Fig. 1) were calculated by using Eq. (4b), using the parameters of CNT in Table I, except that λ was set to 1.774×10^7 K/W. Figure 4 shows a curve separating the square into two areas. If the structural parameters of the CNT fall in the upper area (with white filling), a breakdown event may be caused by thermal runaway.

TABLE I. The parameters used in simulation, determined by matching with Purcell's experimental data.

k (W/mK)	ρ_0 (Ωm)	α (K^{-1})	β (K^{-1})	Φ (eV)	λ (K/W)
100	3.26×10^{-5}	8.5×10^{-4}	9.8×10^{-6}	5.1	1.774×10^7

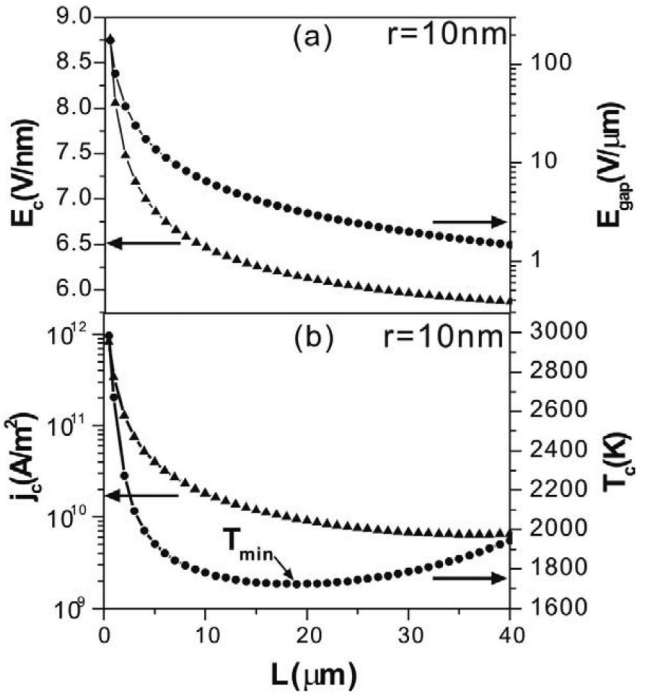

FIG. 3. Length dependence of critical field E_c and applied field E_{gap} (a), and critical current density j_c and critical temperature T_c (b).

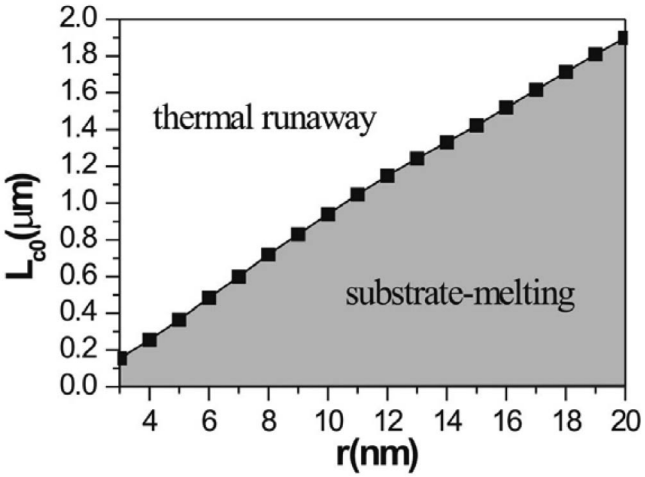

FIG. 4. Showing how the structural parameters of CNT influence failure of a CNT emitter located on a Si tip apex.

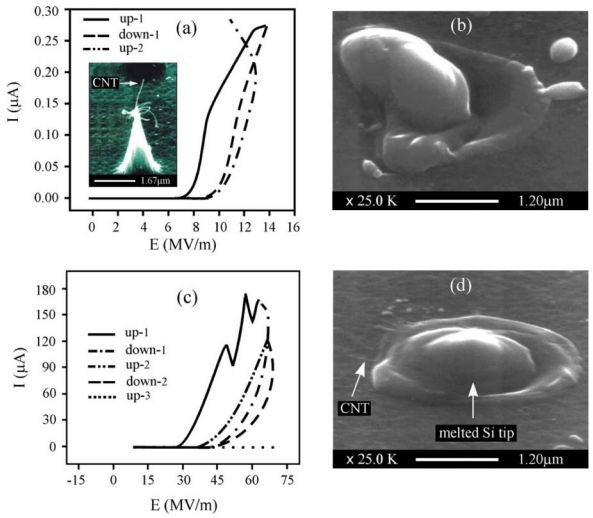

FIG. 5 (color online). *I-E* curves [(a) and (c)] of several test cycles just before failure: (a) $L = 1$ μm, $r = 3$ nm, (c) $L = 1$ μm, $r = 20$ nm. Inset of (a) is the corresponding SEM image of the CNT emitter. (b) and (d) are the corresponding SEM images of the failure sites. (See also Ref. [21]).

Otherwise, a CNT-microtip regime will undergo a substrate-melting process.

This CNT-microtip regime serves as a good structure for experimentally verifying our theory. A procedure was developed to fabricate such structures [21]. For the CNT with $L = 1$ μm and $r = 3$ nm [inset of Fig. 5(a)] falling in the white filling area of Fig. 4, thermal runaway occurred. The *I-E* curves [Fig. 5(a)] explain how the process was progressing [21]. These are marked as up-1, down-1, and up-2. From the up-1 to the down-1, the CNT experienced conditioning. In the following, the low emission current region of the up-2 has a similar behavior to that of the down-1. When the emission increased up to $\sim$0.22 μA, it started to runaway, showing a negative resistance behavior apparent in the high field region of the up-2. Also, the scanning electron microscopy (SEM) image [Fig. 5(b)] shows typical morphological features of a vacuum breakdown site. These findings demonstrated the proposed thermal runaway is a mechanism responsible for initiating a vacuum breakdown process of a CNT emitter.

For another CNT with $L = 1$ μm and $r = 20$ nm, its structural parameters fall in the gray filling area of Fig. 4. No current runaway phenomenon was observed but a slow current decreasing process was recorded: as indicated in the up-1 [Fig. 5(c)], a maximum current was reached, and then the emission current started to decrease though the field was increasing. In the down-1, all of emission current are smaller then those in the up-1. A similar current decreasing trend was observed in the following test cycle. Finally, after the down-2 test, no more current could be detected. SEM inspection indicated that a melted Si mound was left after the test [Fig. 5(d)], and that the CNT still existed nearby the melted Si debris.

In summary, we have shown that thermal runaway is a mechanism responsible for initiating a CNT vacuum breakdown. The underlying physics is the inability of dissipating the heat generated in a positive feedback process. Critical conditions for initiating thermal runaway are dependent of structural and boundary factors. The calculated results are in good accordance with experimental findings.

N. S. X., S. Z. D., and J. C. thank for the financial support from Chinese NSF, MOST and MOE, DOST, and DOE of Guangdong Province and DOST of Guangzhou City.

*Corresponding author.
Email address: stsxns@zsu.edu.cn

[1] S. Iijima., Nature (London) **354**, 56 (1991).
[2] Walt A. de Heer, A. Châtelain, and D. Ugarte, Science **270**, 1179 (1995).
[3] W. B. Choi *et al.*, Appl. Phys. Lett. **75**, 3129 (1999).
[4] N. de Jonge, Y. Lamy, K. Schoots, and T. H. Oosterkmp, Nature (London) **420**, 393 (2002).
[5] P.V. Semet *et al.*, Appl. Phys. Lett. **81**, 343 (2002).
[6] J. M. Bonard, C. Klinke, K. A. Dean, and B. F. Coll, Phys. Rev. B **67**, 115406 (2003).
[7] Z. L. Wang, P. Poncharal, and W. A. de Heer, Appl. Phys. Lett. **80**, 856 (2002).
[8] K. A. Dean, T. P. Burgin, and B. R. Chalamala, Appl. Phys. Lett. **79**, 1873 (2001).
[9] S. T. Purcell, P. Vincent, C. Journet, and V. T. Binh, Phys. Rev. Lett. **88**, 105502 (2002).
[10] P. Vincent, S. T. Purcell, C. Journet, and V. T. Binh, Phys. Rev. B **66**, 075406 (2002).
[11] S. B. Lee *et al.*, Microelectron. Eng. **61/62**, 475 (2002).
[12] T.W. Ebbesen *et al.*, Nature (London) **382**, 54 (1996).
[13] Huang Kun and Han Ruqi, *Solid State Physics* (High Education Press, Beijing, 1988).
[14] P. G. Collins *et al.*, Phys. Rev. Lett. **86**, 3128 (2001).
[15] E. L. Murphy and R. H. Good, Jr., Phys. Rev. **102**, 1464 (1956).
[16] Cai Dayong and Bei Fengshan, *Advanced Numerical Analysis* (Tsinghua University Press, Beijing, 1997).
[17] A. Bachtold *et al.*, Nature (London) **397**, 673 (1999).
[18] D. J. Yang *et al.*, Phys. Rev. B **66**, 165440 (2002).
[19] J. Hone, M. Whitney, C. Piskoti, and A. Zettl, Phys. Rev. B **59**, 2514 (1999).
[20] N. S. Xu and R.V. Latham, in *High Voltage Vacuum Insulation*, edited by R.V. Latham (Academic Press, London, 1995), Chap. 5.
[21] J. C. She *et al.*, Appl. Phys. Lett. **83**, 2671 (2003).